Modeling and Identification of Vibrations in a UAV for Aerial Manipulation

Silvio Cocuzza[1] and Alberto Doria[1]

[1] Department of Industrial Engineering, University of Padova, 35131 Padova, Italy
silvio.cocuzza@unipd.it, alberto.doria@unipd.it

Abstract. Aerial manipulators have many important application scenarios, such as inspection and maintenance, search and rescue, structure assembly, and logistics. One important challenge in aerial manipulation is related to the vibrations induced on the manipulator and its end-effector by the Unmanned Aerial Vehicle (UAV), which significantly affect the grasping and manipulation precision/performance. In this paper, vibration analysis of a heavy payload octocopter has been carried out using Experimental Modal Analysis (EMA). A simplified Mass-Spring-Damper (MSD) dynamic model of the system has then been proposed, whose dynamic parameters have been identified by analyzing selected experimental modes of vibration. The identified model will be useful for the design of the manipulator and related vibrations isolation system.

Keywords: Aerial Manipulator, Vibrations, Experimental Modal Analysis, Identification, Mass-Spring-Damper Model.

1 Introduction

Aerial manipulation is a new and emerging field of research [1]. Aerial manipulators (i.e., rotary-wing Unmanned Aerial Vehicles (UAVs) augmented with a robotic manipulator) have many important potential application scenarios, such as (i) inspection and maintenance (e.g., in the offshore or nuclear industry), (ii) search and rescue in case of a disaster or in hazardous environment, (iii) structure assembly (one or more cooperative aerial manipulators), and (iv) logistics (e.g., in industrial environment). One important challenge in aerial manipulation is related to the vibrations induced on the manipulator and its end-effector by the UAV, which significantly affect the grasping and manipulation precision/performance.

Vibrations in UAVs have been studied in the literature since many years, because they can affect the accuracy of accelerometers and gyroscopes used for their control (and therefore their flight stability) [2, 3], and also because they can affect the quality of images captured with onboard vision systems [4]. In particular, in [2] propellers are identified as the main source of vibrations and numerical simulations of the vibrations on a hexacopter structure using a Finite Elements (FE) model are compared with results obtained using Experimental Modal Analysis (EMA), with a good match between experimental and numerical results. In [5] it has been demonstrated that an

accurate balancing of the propeller blades may significantly reduce the propeller-induced vibrations. The vibrations which appears during the rotation of quadcopters around roll or/and pitch axis are analyzed in [6], and it is demonstrated that these vibrations can be eliminated by using doubled propellers. The performance of different types of dampers for minimizing structural vibrations in UAVs are compared in [3]. A T-type damper for vibration isolation of a UAV mounted radar system is proposed and experimentally validated in [7]. In [8] an active camera mount system using an inertial piezostack actuator in the conventional rubber mount for controlling unwanted vibrations in a UAV is proposed and experimentally validated. In [9] it is demonstrated that propeller induced structural resonance of quadrotor UAVs can be avoided by optimizing the lengths, diameters, and initial and final fiber orientation angles of the arms and landing gears. In [4] the main vibration sources in UAVs are analyzed and a survey of the available methodologies for designing a stabilized optical imaging system is presented. The vibration analysis of an aerial manipulator has not been carried out yet. Nevertheless, methods have been already developed for the identification of joint stiffness of a manipulator using EMA [10], and for minimization of the dynamic disturbances transferred by a manipulator to a moving base [11, 12], which can be useful for the reduction/control of vibrations in aerial manipulators.

In this paper, the vibrations analysis of a heavy payload octocopter has been carried out using EMA, and a simplified Mass-Spring-Damper (MSD) dynamic model of the system has been proposed, whose dynamic parameters have been identified by analyzing selected experimental modes of vibration. The identified model will be useful for the design of the manipulator and related vibrations isolation system, with particular attention to the reduction/control of vibrations at the end-effector.

2 Tested UAV

The UAV considered in this work is a DJI S1000 heavy payload octocopter (Fig. 1). It is composed of (i) a main body, which comprises the eight arms carrying the motors and propellers, (ii) a suspended body, composed by a plate to which the battery is fixed and that will be used as mechanical interface to the robot manipulator, (iii) an

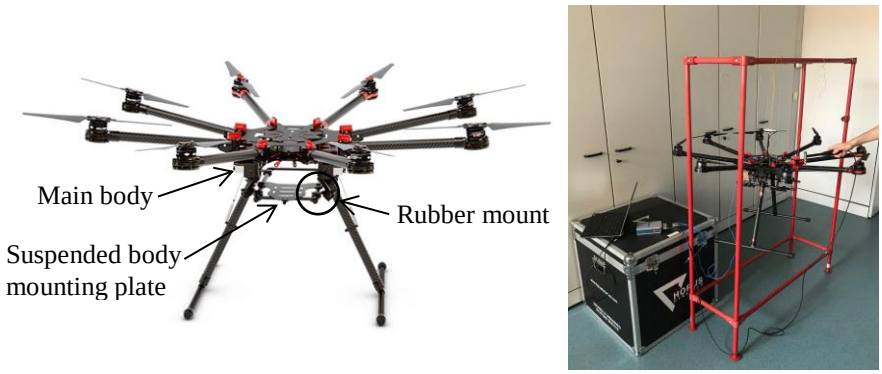

Fig. 1. DJI S1000 octocopter (sx) and experimental setup (dx).

isolation system, composed by four rubber mounts, and (iv) a landing gear composed by two retractable legs.

3 Testing equipment and methods

Experimental results obtained by EMA in the laboratory should be representative of the actual behavior of the system under testing [13], in this specific case of UAV vibrations during typical operations. Since the focus of this research is on aerial manipulation, the UAV was suspended from a structure by means of four small ropes. This solution makes it possible: to support the weight of the UAV without any contact with the ground; to isolate the UAV from sources of excitation other than the hammer blow used for modally testing the system; to minimize the added constraints. Actually, the four ropes generate pendulum motions of the system, but they are low frequency and are well separated from the "true" modes of the UAV.

Excitation was performed by means of a hammer for modal testing (PCB 086C03, sensitivity 2.351 mV/N), and the response of the UAV was measured by means of a triaxial accelerometer (PCB 356A17, sensitivity 50 mV/(m/s^2) in the three directions). Since the UAV is a fully 3D system, a 3D modal model has to be obtained from the experimental tests. Thus, a rowing response modal analysis was carried out moving the triaxial accelerometers to 66 points located in the arms, main body, and suspended body of the UAV. Experimental data were acquired by means of a NI 9234 board and modal analysis was carried out by means of the ModalVIEW software.

4 Experimental results

To give an example of the measured Frequency Response Functions (FRFs), the modulus and the phase of the direct point FRF [14] are represented in Fig. 2a and 2b, respectively.

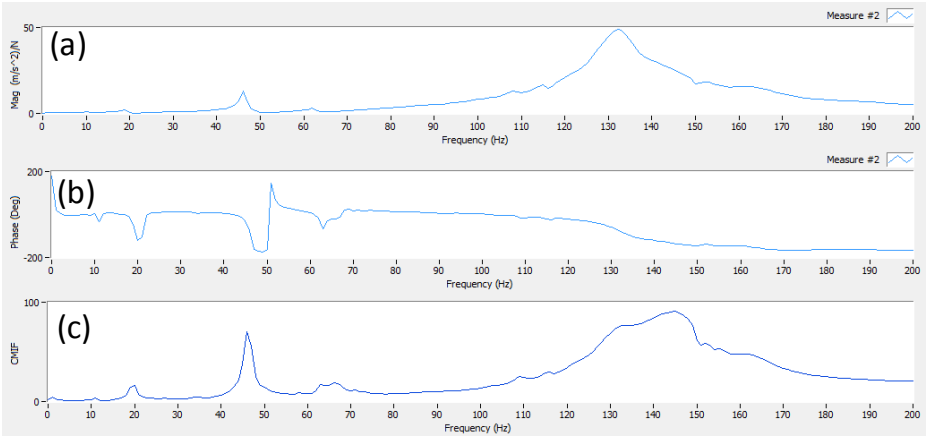

Fig. 2. Direct point FRF (modulus (a) and phase(b)) and CMIF of the measured FRFs (c).

In the range of frequencies 0÷200 Hz the modulus plot shows some clear peaks and the phase plot shows large phase variations at the same frequencies. These phenomena highlight the presence of modes of vibration of the UAV.

A preliminary analysis of the 198 measured FRFs was made using the Complex Mode Indicator Function (CMIF) [14]. The CMIF plot (Fig. 2c) highlights the presence of modes of vibration at about 20, 45, 65 and 140 Hz. There are also small peaks in the range 0÷10 Hz, which are related to pendulum modes of the UAV caused by the ropes of the suspension system. Thus, modal analysis was carried out in the range of frequencies characterized by the largest values of the CMIF function; results are summarized in Table 1.

Table 1. Identified modal properties.

Mode	Frequency [Hz]	Damping ratio	Type
1	19.57	2.668%	Main body and suspended body in opposition
2	46.17	1.303%	Main body and motors in opposition
3	63.02	0.8385%	Torsion

The first mode of vibration of the UAV (19.57 Hz), which is depicted in Fig. 3, is characterized by the relative motion between the main body and the suspended body, which vibrate in phase opposition. Thus, this mode is strongly influenced by the deformability of the rubber mounts; the rather large value of damping ratio corroborates this hypothesis.

Fig. 4 shows that in the second mode of vibration (46.17 Hz) the suspended body is practically steady, whereas there is a large relative motion between the main frame and the motors, which vibrate in phase opposition. All the motors vibrate in the same way owing to the deformability of the arms and of the joints (between the arms and the main body). The third mode of vibration (63.02 Hz) is depicted in Fig. 5; it is dominated by torsion deformation of the arms. Above 100 Hz there is a cluster of modes, which are more complex than the above-mentioned modes. Typically, these modes show large displacements of the arms and negligible displacements of the suspended body.

This research focuses on aerial manipulation and the main aim is the isolation of the base of the robot (which is the suspended frame) from UAV vibrations. Therefore, the high frequency modes of vibration are not a main concern, and the rest of the paper will deal with modeling and controlling the low frequency modes, with relevant displacements of the suspended body.

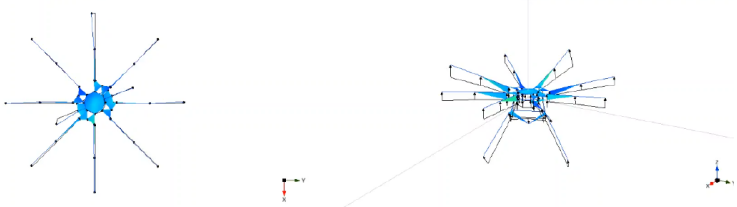

Fig. 3. First mode of vibration (19.57 Hz).

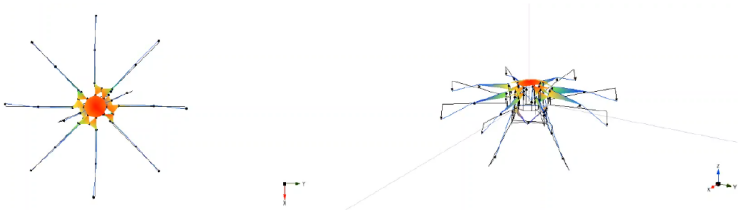

Fig. 4. Second mode of vibration (46.17 Hz).

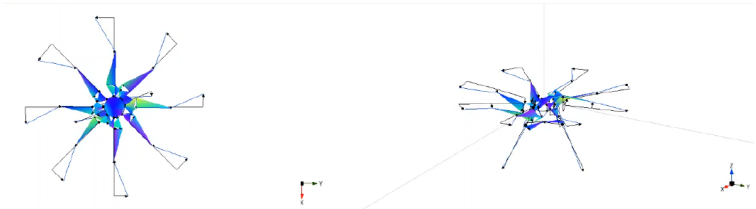

Fig. 5. Third mode of vibration (63.02 Hz).

5 Dynamic models

Two planar MSD models (sections 5.1 and 5.2) are proposed in order to represent the UAV dynamic behaviour related to the first two modes of vibration, and to identify the related stiffnesses and dampings. A third planar model (section 5.3) has then been proposed to validate the method with respect to experimental data.

The dynamic equation describing the dynamics of the MSD models is:

$$[M]\{\ddot{z}\} + [K]\{\dot{z}\} + [C]\{z\} = \{0\} \tag{1}$$

in which $[M]$, $[K]$, and $[C]$ are the mass, stiffness, and damping matrices, respectively. The natural pulsations will be computed using the equation:

$$det\left[[K] - (\omega_n)^2[M]\right] = 0 \tag{2}$$

5.1 1-Degree-Of-Freedom (1-DOF) model

This model (Fig. 6) well represents the first mode of vibration (19.57 Hz) in which the main body and suspended body move in phase opposition. M_d = 3.33 kg, M_m = 1.37 kg, M_b = 2.33 kg are the drone, motors, and base masses, respectively, and K_z, C_z the stiffness and damping.

The mass, stiffness, and damping matrixes to be used in Eq. (1) are:

$$[M] = \begin{bmatrix} M_d + M_m & 0 \\ 0 & M_b \end{bmatrix}, \quad [K] = \begin{bmatrix} K_z & -K_z \\ -K_z & K_z \end{bmatrix}, \quad [C] = \begin{bmatrix} C_z & -C_z \\ -C_z & C_z \end{bmatrix} \tag{3}$$

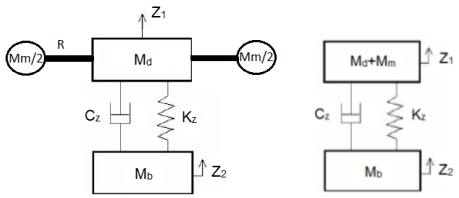

Fig. 6. 1-DOF model (first mode of vibration).

Using Eq. (2), and discarding the solution ω_{n1}= 0, it is possible to find:

$$\omega_{n2} = \sqrt{\frac{K_z}{m_{eq}}}, \text{ with } m_{eq} = \frac{(M_m+M_d)M_b}{(M_m+M_d+M_b)} \tag{4}$$

Considering ω_{n2} = 19.57*2π rad/s, it is possible to compute K_z= 23560 N/m. The damping ratio ζ = 0.02668 (from EMA) can also be expressed as:

$$\zeta = \frac{C_z}{2\sqrt{K_z m_{eq}}} \tag{5}$$

Therefore, the value of C_z= 10.22 Ns/m can be computed from Eq (5).

5.2 2-DOFs model

This model well represents the second mode of vibration (46.17 Hz), in which the suspended body stands still, and the main body and motors move in phase opposition. Fig. 7 shows only two motors, but the model does not change if eight motors move in phase. K_z and C_z are the stiffness and damping computed in section 5.1. The arms deformation is concentrated at their attachment with the UAV frame, therefore the equations

$$K_{eq} = K_\theta/R^2,\ C_{eq} = C_\theta/R^2 \tag{6}$$

with R = 0.386 m (arm length) and $z_2 = R\theta$, allow to switch from arm rotational stiffness and damping (K_θ, C_θ, Fig. 7 (sx)) to equivalent arm linear stiffness and damping (K_{eq}, C_{eq}, Fig. 7 (dx)).

The mass, stiffness, and damping matrixes to be used in Eq. (1) are:

$$[M] = \begin{bmatrix} M_d & 0 \\ 0 & M_m \end{bmatrix},\ [K] = \begin{bmatrix} K_z + K_{eq} & -K_{eq} \\ -K_{eq} & K_{eq} \end{bmatrix},\ [C] = \begin{bmatrix} C_z + C_{eq} & -C_{eq} \\ -C_{eq} & C_{eq} \end{bmatrix} \tag{7}$$

Using the experimental value of the natural frequency (46.17 Hz) in Eq. (2), it is possible to compute K_{eq} = 79492 N/m. Substituting the value of K_{eq} back in Eq. (2), it is possible to find the second natural frequency (11.12 Hz) and the eigenvectors and modal matrix $[U]$ (its columns are the eigenvectors), which diagonalizes the mass, stiffness, and damping matrices:

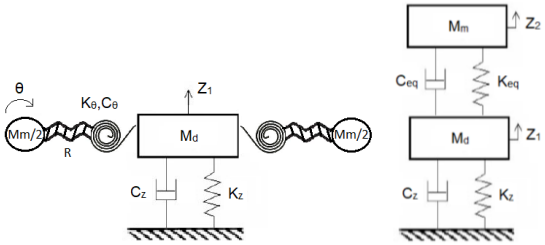

Fig. 7. 2-DOFs model (second mode of vibration).

$$[M_D] = [U]^t[M][U], \;\; [K_D] = [U]^t[K][U], \;\; [C_D] = [U]^t[C][U] \tag{8}$$

Using the element $M_D(2,2)$ of matrix $[M_D]$, the element $K_D(2,2)$ of matrix $[K_D]$, and the experimental damping ratio $\zeta = 0.01303$ for the second mode, it is possible to find the element $C_D(2,2)$ of matrix $[C_D]$

$$C_D(2,2) = 2\zeta\sqrt{K_D(2,2)M_D(2,2)} \tag{9}$$

and substituting this value in Eq. (8) ($[C_D] = [U]^t[C][U]$), it is possible to find C_{eq} = 6.365 Ns/m.

5.3 3-DOFs model

Using the values of K_z, C_z, K_{eq}, C_{eq} identified in sections 5.1 and 5.2, it is possible to assemble a 3-DOFs model of the UAV with suspended body (Fig. 8).

The mass, stiffness, and damping matrixes to be used in Eq. (1) are:

$$[M] = \begin{bmatrix} M_d & 0 & 0 \\ 0 & M_b & 0 \\ 0 & 0 & M_m \end{bmatrix}, \;\; [K] = \begin{bmatrix} K_z + K_{eq} & -K_z & -K_{eq} \\ -K_z & K_z & 0 \\ -K_{eq} & 0 & K_{eq} \end{bmatrix}, \;\; [C] = \begin{bmatrix} C_z + C_{eq} & -C_z & -C_{eq} \\ -C_z & C_z & 0 \\ -C_{eq} & 0 & C_{eq} \end{bmatrix} \tag{10}$$

Using Eq. (2), the eigenfrequencies of this system are computed, which have an error less than 1.5% with respect to the experimental ones, and this validates the model.

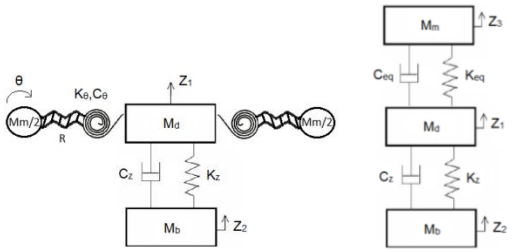

Fig. 8. 3-DOFs model.

6 Conclusions

EMA has shown that the rubber mounts are able to isolate the base of the manipulator (suspended body) from UAV vibrations above 50 Hz. A 3-DOFs MSD dynamic model of the UAV has been proposed, whose dynamic parameters have been identified by analyzing selected experimental modes of vibration. The identified model will be useful for the design of the manipulator to be mounted on the UAV.

References

1. Ruggiero, F., Lippiello, V., Ollero, A.: Aerial manipulation: A literature review. IEEE Robotics and Automation Letters, 3(3), 1957-1964 (2018).
2. Verbeke, J., Debruyne, S.: Vibration analysis of a UAV multirotor frame. Proceedings of ISMA 2016 - International Conference on Noise and Vibration Engineering (2016).
3. Li, Z., Lao, M., Phang, S.K., Hamid, M.R.A., Tang, K.Z., Lin, F.: Development and Design Methodology of an Anti-Vibration System on Micro-UAVs. Proceedings of the International Micro Air Vehicle Conference and Flight Competition, Toulouse, France (2017).
4. Dahlin Rodin, C., de Alcantara Andrade, F.A., Hovenburg, A.R., Johansen, T.A.: A Survey of Practical Design Considerations of Optical Imaging Stabilization Systems for Small Unmanned Aerial Systems. Sensors, 19(21), (2019).
5. Mizui, M., Yamamoto, I., Ohsawa, R.: Effects of propeller-balance on sensors in small-scale unmanned aerial vehicle. IOSRJEN, 2, 23-27 (2012).
6. Radkowski, S., Szulim, P.: Analysis of vibration of rotors in unmanned aircraft. Advances in Intelligent Systems and Computing, 317, 363-371 (2015).
7. Changshuai, Y., Haitao, L., Siwei, G.: Vibration test and vibration reduction design of UAV load radar. ACM International Conference Proceeding Series, (2019).
8. Oh, J.-S., Han, Y.-M., Choi, S.-B.: Vibration control of a camera mount system for an unmanned aerial vehicle using piezostack actuators. Smart Materials and Structures, 20(8), (2011).
9. Tullu, A., Byun, Y., Kim, J.-N., Kang, B.-S.: Parameter optimization to avoid propeller-induced structural resonance of quadrotor type Unmanned Aerial Vehicle. Composite Structures, 193, 63-72 (2018).
10. Doria, A., Cocuzza, S., Comand, N., Bottin, M., Rossi, A.: Analysis of the compliance properties of an industrial robot with the Mozzi axis approach. Robotics, 8(3), (2019). DOI: 10.3390/robotics8030080.
11. Cocuzza, S., Pretto, I., Debei, S.: Least-squares-based reaction control of space manipulators. Journal of Guidance, Control, and Dynamics, 35(3), 976-986 (2012). DOI: 10.2514/1.45874.
12. Cocuzza, S., Tringali, A.: Extended reactionless workspace of a space manipulator through reaction wheels. Proceedings of the International Astronautical Congress, IAC, (2018).
13. Cossalter, V., Doria, A., Basso, R., Fabris, D.: Experimental analysis of out-of-plane structural vibrations of two-wheeled vehicles. Shock and Vibration, 11(3-4), 433-443, (2004). DOI: 10.1155/2004/905629.
14. Ewins, D. J. Modal testing: theory, practice and application 2nd edn., Research Studies Press LTD, Baldock UK, (2000).